British Journal of Pharmacology

British Journal of Pharmacology (2016) **173** 1438–1451 1438

RESEARCH PAPER

Hippocampal 5-HT$_7$ receptors signal phosphorylation of the GluA1 subunit to facilitate AMPA receptor mediated-neurotransmission *in vitro* and *in vivo*

Correspondence Professor Nicholas Barnes, Clinical and Experimental Medicine, College of Medical and Dental Sciences, University of Birmingham, Edgbaston, Birmingham, B15 2TT, UK. E-mail: n.m.barnes@bham.ac.uk

Received 24 July 2015; **Revised** 21 December 2015; **Accepted** 12 January 2016

Filippo Andreetta[1,2*†], Lucia Carboni[2*‡], Gillian Grafton[1], Ross Jeggo[3], Andrew D Whyment[3], Marco van den Top[3], Daniel Hoyer[4,5,6], David Spanswick[3] and Nicholas M Barnes[1,4]

[1]Clinical and Experimental Medicine, College of Medical and Dental Sciences, University of Birmingham, Edgbaston, Birmingham, UK, [2]Neurosciences CEDD, GlaxoSmithKline Medicine Research Centre, Verona, Italy, [3]NeuroSolutions Limited, Coventry, UK, [4]Department of Pharmacology and Therapeutics, School of Biomedical Sciences, Faculty of Medicine, Dentistry and Health Sciences, The University of Melbourne, Parkville, Vic. Australia, [5]The Florey Institute of Neuroscience and Mental Health, The University of Melbourne, 30 Royal Parade, Parkville, Victoria 3052, Australia, and [6]Department of Chemical Physiology, The Scripps Research Institute, 10550 N. Torrey Pines Road, La Jolla, CA 92037, USA

*Joint first authors.

†Present address: Aptuit srl., Medicine Research Centre, Verona, Italy

‡Present address: Department of Pharmacy and Biotechnology, Alma Mater Studiorum University of Bologna, Bologna, Italy

BACKGROUND AND PURPOSE

The 5-HT$_7$ receptor is a GPCR that is the target of a broad range of antidepressant and antipsychotic drugs. Various studies have demonstrated an ability of the 5-HT$_7$ receptor to modulate glutamatergic neurotransmission and cognitive processes although the potential impact upon AMPA receptors has not been investigated directly. The purposes of the present study were to investigate a direct modulation of the GluA1 AMPA receptor subunit and determine how this might influence AMPA receptor function.

EXPERIMENTAL APPROACH

The influence of pharmacological manipulation of the 5-HT$_7$ receptor system upon phosphorylation of GluA1 subunits was assessed by Western blotting of fractionated proteins from hippocampal neurones in culture (or proteins resident at the neurone surface) and the functional impact assessed by electrophysiological recordings in rat hippocampus *in vitro* and *in vivo*.

KEY RESULTS

5-HT$_7$ receptor activation increased cAMP and relative pCREB levels in cultures of rat hippocampal neurones along with an increase in phosphorylation (Ser845) of the GluA1 AMPA receptor subunit evident in whole neurone extracts and within the neurone surface compartment. Electrophysiological recordings in rat hippocampus demonstrated a 5-HT$_7$ receptor-mediated increase in AMPA receptor-mediated neurotransmission *in vitro* and *in vivo*.

CONCLUSIONS AND IMPLICATIONS

The 5-HT$_7$ receptor-mediated phosphorylation of the GluA1 AMPA receptor provides a molecular mechanism consistent with the 5-HT$_7$ receptor-mediated increase in AMPA receptor-mediated neurotransmission.

Abbreviations

CREB, cAMP response element-binding protein; 5-CT, 5-carboxamidotryptamine; GFAP, glial fibrillary acidic protein; NBQX, 2,3-dihydroxy-6-nitro-7-sulfamoyl-benzo[f]quinoxaline-2,3-dione; pCREB, phosphorylated CREB

DOI:10.1111/bph.13432

Tables of Links

TARGETS	
GPCRs[a]	**Enzymes**[c]
5-HT$_{1A}$ receptor	PDE4
5-HT$_4$ receptor	PDE10
5-HT$_6$ receptor	p38
5-HT$_7$ receptor	PKA
Ligand-gated ion channels[b]	
AMPA receptor	
GluR1, GluA1	

LIGANDS	
5-CT	H89
5-HT	Lurasidone
AMPA	NBQX
AP5	Rolipram
AS-19	SB258719
Bicuculline	SB399885
CGP-55845	Tetrodotoxin
Forskolin	Vortioxetine
GR113808	WAY-100,635

These Tables list key protein targets and ligands in this article which are hyperlinked to corresponding entries in http://www.guidetopharmacology.org, the common portal for data from the IUPHAR/BPS Guide to PHARMACOLOGY (Pawson *et al.*, 2014) and are permanently archived in the Concise Guide to PHARMACOLOGY 2015/16 ([a,b,c]Alexander *et al.*, 2015a,b,c).

Introduction

The 5-HT$_7$ receptor has been cloned from various species and is a member of the GPCR superfamily (Hoyer *et al.*, 1994; Alexander *et al.*, 2015a). The 5-HT$_7$ receptor signals via an increase in cAMP production as well as various other pathways (Shen *et al.*, 1993; see Gellynck *et al.*, 2013) and is the focus of various projects to identify novel therapeutics to treat conditions such as depression, sleep disorders and cognitive deficits (Mnie-Filali *et al.*, 2007). Further clinical interest in the 5-HT$_7$ receptor arises from a broad range of antidepressant and antipsychotic drugs displaying relatively high affinity for the receptor (Roth *et al.*, 1994). Further, two non-selective 5-HT$_7$ receptor antagonists have recently received marketing authorisation for the treatment of psychiatric conditions: lurasidone and vortioxetine (Fountoulakis *et al.*, 2015; Sanchez *et al.*, 2015).

Expression of the 5-HT$_7$ receptor is apparent throughout the body with notable expression in the brain and spinal cord, vascular system and gastrointestinal tract (Waeber and Moskowitz, 1995; Gustafson *et al.*, 1996; Stowe and Barnes, 1998; Neumaier *et al.*, 2001). Within the brain, there is prominent expression within the hippocampus (Waeber and Moskowitz, 1995; Gustafson *et al.*, 1996; Neumaier *et al.*, 2001; Mengod *et al.*, 2010), where homodimerization and heterodimerisation with the 5-HT$_{1A}$ receptor may be relevant (Renner *et al.*, 2012). At the cellular level within the hippocampus, expression in glutamatergic pyramidal neurones is evident (Neumaier *et al.*, 2001), which is consistent with a number of independent studies demonstrating that the 5-HT$_7$ receptor mediates excitation of glutamatergic pyramidal neurones and associated network activity (Bacon and Beck, 2000; Bickmeyer *et al.*, 2002; Gill *et al.*, 2002; Tokarski *et al.*, 2003, 2005; Costa *et al.*, 2012). Such neurophysiological actions may underlie the improvement in cognitive performance following 5-HT$_7$ receptor activation (Meneses, 2004; Perez-Garcia and Meneses, 2005; Eriksson *et al.*, 2008; Freret *et al.*, 2014), which is consistent with the reduced cognitive performance following inhibition of 5-HT$_7$ receptor function by pharmacological antagonism or genetic manipulation (Meneses, 2004; Ballaz *et al.*, 2007; Sarkisyan and Hedlund, 2009; Freret *et al.*, 2014; but see Horisawa *et al.*, 2011 and Waters *et al.*, 2012). However, some types of memory deficit are improved by 5-HT$_7$ receptor antagonists (McLean *et al.*, 2009; Bonaventure *et al.*, 2011; Nikiforuk *et al.*, 2013), which may be a consequence of different neurochemical mechanisms (Bonaventure *et al.*, 2011) or biased signalling; this is consistent with the beneficial effects of some non-selective 5-HT$_7$ receptor antagonists used to treat psychiatric conditions (Horiguchi *et al.*, 2011).

In terms of a molecular mechanism by which the 5-HT$_7$ receptor might drive neuronal excitation in the hippocampus, recent evidence demonstrates that the 5-HT$_7$ receptor mediates phosphorylation of NMDA glutamate receptors with a consequential increase in NMDA receptor signalling (Vasefi *et al.*, 2013). Consistent with these findings, 5-HT$_7$ receptor knock-out mice display reduced LTP in the hippocampus (Roberts *et al.*, 2004). It should be noted, however, that 5-HT$_7$ receptor knock-out mice also display impaired contextual fear conditioning – a hippocampus-dependent phenomenon – but no deficit in spatial learning (Roberts *et al.*, 2004), which implicates 5-HT$_7$ receptor modulation of AMPA receptor neurotransmission (Zamanillo *et al.*, 1999). In support of this, 5-HT$_7$ receptors enhance AMPA receptor-mediated transmission in the hippocampus via an action on postsynaptic neurones (Costa *et al.*, 2012).

In the present study, we have investigated the ability of the 5-HT$_7$ receptor to alter glutamatergic neurotransmission in the hippocampus and have demonstrated that activation of the receptor promotes PKA-mediated phosphorylation of native GluA1 AMPA receptor subunits in rat hippocampus, which results in an increased insertion of the Ser^{845}-phosphorylated GluA1 (pGluA1(Ser^{845}) subunit, into the neuronal membrane. This change is likely to contribute to the observed increase in AMPA receptor-mediated neurotransmission in the hippocampus both *in vitro* and *in vivo*.

Methods

Animals

All animal care and experimental protocols were in accordance with the European Communities Council Directive 2010/63/EU and Italian or UK legislation acts concerning animal experimentation and were approved by the Local Ethics Committees. Efforts were made to minimize animal suffering and to reduce the number of animals used. All *in vivo* experiments were performed and are reported in accordance with the ARRIVE guidelines (Kilkenny *et al.*, 2010; McGrath and Lilley, 2015).

Preparation of rat neurone or astrocyte cultures

Hippocampal predominantly neuronal cultures were obtained from embryos at day 18/19 of gestation (E18/19) of Sprague–Dawley rats (embryos killed by decapitation). Hippocampi were quickly isolated into HBSS [pH 7.3 buffer containing HEPES (10 mM), penicillin (100 U•mL^{-1}) and streptomycin (100 μg•mL^{-1}) 4°C] before incubation of trypsin {0.1%; 37°C, 10 min [for the last 5 min of this incubation, DNAse I (166-μg•mL^{-1}) was added]}, washed with HBSS buffer containing 10% FBS and cells dissociated by triturating. Cells were placed in poly-L-lysine (MW >30 000 kDa)-coated plates (density of 700–800 cells•mm^{-2}) in serum-free NEUROBASAL™ Medium supplemented with B-27® Supplement, glutamine (500 μM), glutamate (12.5 μM), penicillin (100 U•mL^{-1}) and streptomycin (100 μg•mL^{-1}). Cells were grown at 37°C, 5% CO_2, and half the volume of the medium was replaced after 4 days with complete medium minus glutamate. For all assays, primary cells were used between 8 and 10 days in culture.

Phenotype and purity of cell cultures

Purity of cultured cells was assessed by phenotyping with primary antibodies {rabbit anti-glial fibrillary acidic protein (GFAP); 1:1000 (Sigma-Aldrich) or anti-NeuN [mouse 1:200 (Chemicon; Merck Millipore (Darmstadt, Germany))]}, with five fields per coverslip acquired using a Leica (Wetzlar, Germany) microscope (IM 50 programme; 20× objective) with positive cells counted manually.

RNA extraction and quantification

Total RNA from cultured cells was extracted using RNeasy mini kit from Qiagen (Qiagen Inc, Valencia, CA, USA) following the manufacturer's instructions. Genomic DNA was removed using RNAse-free DNase I (Applied Biosystems, Life Technologies). Purified RNA was quantified using an Agilent 2100 Bioanalyzer following the Agilent RNA 6000 Nano kit protocol (Agilent Technologies Inc).

Reverse transcribed PCR

cDNA was generated by reverse transcription of total RNA (100 ng) using TaqMan Reverse Transcription Reagents (Applied Biosystems, Life Technologies): 1× reverse transcription buffer, $MgCl_2$ (2.5 mM), deoxynucleotides (1 mM), random hexamers (2.5 μM), RNase inhibitor (0.4 U•μL^{-1}) and MultiScribe Reverse Transcription (1.25 U•μL^{-1}). The mixture was incubated consecutively at 25 (10 min), 48 (30 min) and 95°C (5 min). PCR was performed using HotStarTaq(R) PCR from Qiagen: 10 ng cDNA, 1× PCR buffer, 200 μM deoxynucleotides, 300 nM Primers, 1 unit Taq in DNase-free water. After 15 min incubation (95°C), 40 cycles of amplification were performed (30 s denaturation at 95°C, 30 s annealing at 60°C and 40 s extension at 72°C) before termination with 10 min extension at 72°C. Primer pairs were as follows:

5-HT$_7$ receptor:

Forward: ATCTTCGGCCACTTCTTCTGCAACG
Reverse: CAGCACAAACTCGGATCTCTCGGG

5-HT$_6$ receptor:

Forward: CCATCTGCTTCACCTACTGC
Reverse: TCTGAATCTGAGTTTGGCGG

5-HT$_4$ receptor:

Forward: TTGGCTGCTTTGGTCTCTGTCCGC;
Reverse: TGCAAGGCTGGAACAACATCGGC.

PCR products were separated electrophoretically [1.5% agarose gels in 1× Tris acetate EDTA buffer (Tris 40 mM, glacial acetic acid 1 mM, 0.1% EDTA, pH 8)] with SYBR safe DNA gel stain (Invitrogen, Life Technologies) running alongside DNA MW markers (100 bp ladder; Invitrogen, Life Technologies) for 1 h at 100 V.

Assessment of cAMP concentration

cAMP was quantified using the cAMP Hi Range kit (Cisbio, Bagnois-sur-Ceze, France) according to the manufacturer's instructions.

Sample preparation and measurement of total CREB, pCREB, and phospho-p38 MAPK

Cells were removed by scraping in lysis buffer [Tris (10 mM; pH 7.4), NaCl (100 mM), EDTA (1 mM), EGTA (1 mM), NaF (1 mM), $Na_4P_2O_7$ (20 mM), Na_3VO_4 (2 mM), 1% Triton X-100, 10% glycerol, 0.1% sodium dodecyl sulfate, 0.5% deoxycholate, PMSF (2 mM), protease inhibitors (Complete Mini, Roche Life Science, Sigma-Aldrich) and 1% phosphatase inhibitors I and II (Sigma-Aldrich)]. Cells lysates were incubated at 4°C for 30 min before centrifugation (10 min at 13 000 × *g*) and the supernatants quantified for total cAMP response element-binding protein (CREB) and Ser^{133}-phosphorylated CREB (pCREB) by ELISA (Invitrogen, Life Technologies) according to the manufacturer's instructions. Phosphorylated p38 MAPK levels were also measured by ELISA (Cell Signaling Technology, Beverley, CA, USA) following the manufacturer's instructions.

Isolation of cell surface proteins

Cell surface proteins were isolated using EZ-link sulfo-NHS-SS-Biotin (Pierce) at 4°C. Cells were incubated with biotin (1 mg•mL^{-1}; 20 min) and dissolved in PBS. After three rinses in ice-cold glycine (50 mM) in PBS, cells were scraped into homogenization buffer (0.1% sodium dodecyl sulfate, 0.5% NP40, 0.5% sodium deoxycholate, 150 mM NaCl, complete mini protease inhibitors, phosphatase inhibitors cocktail I and II in PBS; pH 7.4) and centrifuged (10 000 × *g*; 20 min), and the supernatant represented the total protein extract.

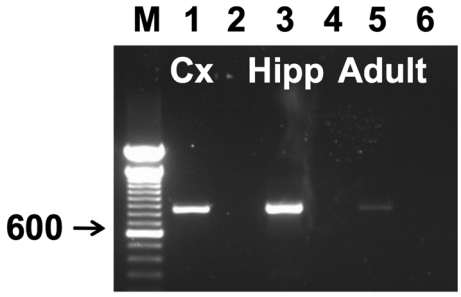

Figure 1

Expression of the 5-HT$_7$ receptor by hippocampal primary cells in culture, compared with the expression by primary cerebral cortex cells and adult rat hippocampal tissue. Representative RT-PCR of cDNA products of around 850 bp from adult rat hippocampi (Adult: lanes 5 and 6) and primary cells cultured from the hippocampi (Hipp: lanes 3 and 4) and cerebral cortices (Cx: lanes 1 and 2) of E18/19 rat embryos. Lanes 2, 4 and 6 show lack of product when the enzyme was omitted from the reverse transcription step. Each line of the ladder (M) represents a band size increase of 100 bp. Similar results were obtained from three independent experiments.

For purification of the biotinylated surface protein fraction, 50 μg of total proteins was incubated with 80 μL of 50% slurry Neutravidin resin (Pierce) for 2 h at 4°C. After washing, biotinylated proteins were eluted [100 μL of elution buffer; Invitrogen NuPage LDS sample buffer with ditiothreitol (50 mM)], heated at 95°C for 5 min before centrifugation (1000 × *g* for 2 min).

Protein concentration was determined using Bio-Rad reagents (Bio-Rad Laboratories Inc., Hercules, CA, USA) based on the Bradford assay. When protein concentration was expected to be low, the micro BCA kit was used (Pierce).

SDS-PAGE Western blotting

Proteins were separated using SDS-PAGE in an XCell SureLock™ Mini-Cell (Invitrogen, Life Technologies). Equal amounts of cell lysates (~6–10 μg protein) in 4× NuPAGE® LDS Sample Buffer and 10× NuPAGE Sample Reducing Agent were boiled for 5 min, centrifuged briefly and loaded in precast gels (1.5 mm 4–12% Novex Bis-Tris Pre-cast Mini Gels; Invitrogen, Life Technologies). Prestained protein MW markers (Novex® Sharp Pre-stained Protein Standard) were loaded in parallel. Electrophoresis was performed (50 V for 1 h), and proteins were transferred to PVDF membranes (Amersham plc, Little Chalfont, Bucks, UK) using a Mini Trans-Blot module (Bio-Rad) in transfer buffer (25 mM Tris, 192 mM Glycine, 20% methanol; pH 8.3) at 40–50 V for 2 h. PVDF membranes were blocked (5% skimmed dried milk in Tris-buffered saline (50 mM Tris HCl, 280 mM NaCl, 2.7 mM KCl, pH 7.6; 1 h) containing 0.1% Tween-20) and then incubated with the relevant primary antibodies; either rabbit anti-pGluA1(Ser^{845}) (Sigma-Aldrich; 1:1000), rabbit anti-GluA1 (Millipore; 1:1000), rabbit anti-pan cadherin (Abcam plc, Cambridge, UK; 1:1000) or mouse anti-GAPDH (Santa Cruz Biotechnology, Santa Cruz, CA, USA; 1:10 000). Membranes were washed (3 × 10 min) with 0.1% Tween-20 in Tris-buffered saline before incubation (1 h at room temperature) with peroxidase-conjugated secondary antibodies (goat anti-rabbit IgG-HRP or goat anti-mouse IgG-HRP, Santa Cruz; 1:5000). The chemiluminescence reaction was developed with ECL Plus (Amersham plc, Little Chalfont, Bucks, UK) and detected with Luminescent Image Analyzer LAS-4000 mini (Fujifilm, Tokyo, Japan). ODs were determined by densitometric analysis with Quantity One software (Bio-Rad).

Electrophysiological recording in the hippocampus in vivo

Adult male Sprague–Dawley rats (250–350 g, n = 12) (Charles River, Margate, UK) were initially anaesthetized with isoflurane and subsequently with chloral hydrate (400 mg•kg^{-1} i.p.) with anaesthetic depth maintained by constant i.v. infusion (80–120 mg•kg^{-1}•h^{-1}) with adjustments, depending on corneal reflex, withdrawal response to paw pinch and the stability of monitored cardiovascular variables. Core body temperature was maintained at 37 ± 1°C. The right femoral vein, the artery and the trachea were cannulated to permit respectively the

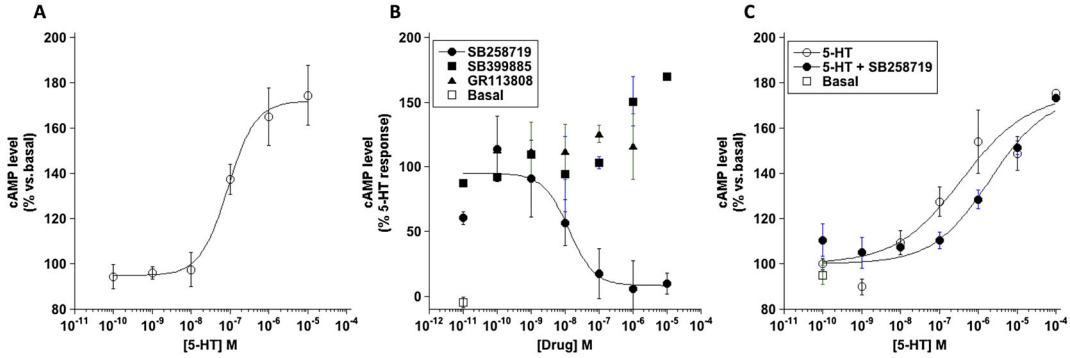

Figure 2

Ability of the 5-HT$_7$ receptor to increase cAMP levels in hippocampal neurones. (A) Concentration-dependent ability of 5-HT to increase intracellular cAMP levels. (B) Concentration-dependent ability of the selective 5-HT$_7$ receptor antagonist, SB258719, to inhibit the 5-HT (100 nM)-induced increase in cAMP levels and lack of inhibition by the selective 5-HT$_4$ and 5-HT$_6$ receptor antagonists (GR113808 and SB399885 respectively). Data represent the percentage of cAMP increase after 5-HT addition versus basal levels (mean ± SEM, n = 3). (C) Concentration-dependent ability of 5-HT to increase intracellular cAMP levels in the absence and presence of the selective 5-HT$_7$ receptor antagonist, SB258719 (100 nM); the rightward shift in the 5-HT concentration–response curve is indicative of competitive antagonism by SB258719. Data represent mean ± SEM, n = 3.

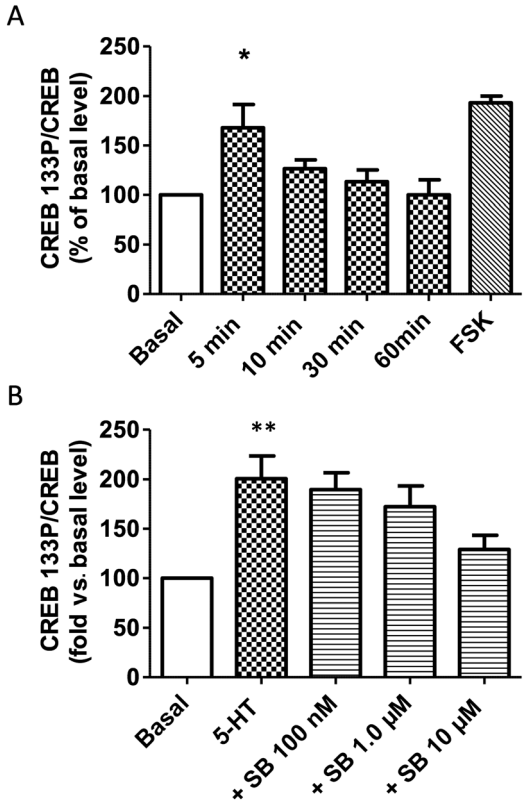

Figure 3

Ability of the 5-HT$_7$ receptor to increase CREB phosphorylation in hippocampal neurones. (A) Time-dependent effect of 5-HT (1 μM) upon CREB phosphorylation [forskolin (10 μM) applied for 30 min]. Data were the mean ± SEM of eight [5-HT (5 min)] or three [5-HT (10–60 min) or forskolin (FSK)] independent experiments and represent the pCREB/total CREB ratio of treated cells versus basal levels. *$P < 0.05$, **$P < 0.01$ 5-HT (5 min) versus basal levels; Mann–Whitney *U*-test. (B) Concentration-dependent ability of the selective 5-HT$_7$ receptor antagonist, SB258719, to inhibit 5-HT (1 μM; 5 min)-induced CREB phosphorylation. Data represent the mean ± SEM from three independent experiments.

administration of supplemental anaesthetic, the recording of arterial BP via a pressure transducer and amplifier (Neurolog module NL108; Digitimer, Welwyn Garden City, UK) and the maintenance of a clear airway. Animals were placed in a stereotaxic frame (Narishige ST-7) and the dorsal brain surface overlying the hippocampus exposed by craniotomy. A small incision was made in the dura, and a multibarrel recording electrode (Kation Scientific, Minneapolis, MN, USA) was lowered vertically through the cortex to the CA3 pyramidal layer of the hippocampus according to the following stereotaxic boundaries (Paxinos and Watson, 1998): Bregma −3.9 to 4.4 mm, lateral 3.7–4.2 mm and depth 3.6–4.2 mm below pial surface. Unitary activity was recorded through an extracellular carbon fibre microelectrode, and using the Neurolog system, the signal was amplified (×10 k, module NL104) and filtered (bandwidth 1–30 kHz, module NL125), with the conditioned output being captured on a PC using a micro1401 interface with Spike 2 software (CED). Multibarrel electrodes were filled with 5-carboxamidotryptamine (5-CT) (DP-5-CT, 1–10 mM), WAY-100,635 (1–10 mM), AMPA (5 mM in 195 mM NaCl; pH 8) and 2,3-dihydroxy-6-nitro-7-sulfamoyl-benzo[f]quinoxaline-2,3-dione (NBQX) (disodium salt, 1 mM in double distilled H_2O; pH 8) and for current balancing and recording site marking, Chicago Sky Blue. Initially, baseline CA3 pyramidal neurone activity was examined during iontophoretic administration of 5-CT alone and in the presence of the 5-HT$_{1A}$ receptor antagonist WAY-100,635. Subsequent experiments examined the response to 5-CT, with and without concomitant application of WAY-100,635, on neuronal bursts of firing induced by cyclical (5/30 s) iontophoretic administration of AMPA. NBQX was iontophoretically administered at the end of experiments to confirm that AMPA-induced excitations were selective. Stable baseline or AMPA-evoked neuronal activity was recorded for a minimum of 5 min before test substance examination. Neurones with unstable activity or whose recording location lay outside the pyramidal layer were excluded from analyses. Neuronal activity was measured in spikes per second (Hz) for a minimum period of 60 s before and during test compound treatment.

Subsequent to electrophysiological recordings *in vivo*, rats were killed without recovery of consciousness by an overdose of sodium pentobarbitone (200 mg•kg^{-1}), followed by cervical dislocation.

Electrophysiological recording in the hippocampus in vitro

Male Sprague–Dawley rats (6–8 weeks old) were killed by anaesthetic overdose using isoflurane inhalation. Transverse hippocampal slices (400 μm thickness) were cut using a vibratome (Leica VTS1000) in chilled (<4°C) carbogenated (95% O_2/5% CO_2) artificial CSF (NaCl, 127 mM; KCl, 1.9 mM; KH_2PO_4, 1.2 mM; $CaCl_2$, 2.4 mM; $MgCl_2$, 1.3 mM; $NaHCO_3$, 26 mM; D-glucose, 10 mM). Slices were maintained in artificial CSF at room temperature for a minimum of 1 h before transferring to a custom-built recording chamber to commence whole-cell recordings from hippocampal CA3 pyramidal neurones with an Axopatch 1D amplifier (Molecular Devices LLC, Sunnyvale, CA, USA), using the blind version of the patch clamp technique (Pickering *et al.*, 1991). Patch pipettes were pulled from thin-walled borosilicate glass (GC150-TF10, Harvard Apparatus) with resistances between 3 and 8 MΩ when filled with intracellular solution of the following composition: Kgluconate, 130 mM; KCl, 10 mM; EGTA-Na, 1 mM; HEPES, 10 mM; Na_2ATP, 4 mM; Na_2GTP, 0.3 mM; Lucifer yellow, 2 mM; pH adjusted to 7.4 with KOH and osmolarity adjusted to 310 mOsm with sucrose. Data were filtered at 2–5 kHz (current clamp) or 1 kHz (voltage clamp), digitized at 10 kHz (Digidata 1322; Molecular Devices LLC) and recorded on a PC running Clampex 9.1 software (Molecular Devices LLC). After achieving whole-cell access, current/voltage relations were generated to identify intrinsic membrane conductances consistent with CA3 pyramidal neurones. In voltage clamp experiments, mossy fibre pathway synaptic inputs were stimulated using a concentric bipolar stainless steel electrode and AMPA receptor-mediated EPSCs pharmacologically isolated using D-AP5 (25 μM), bicuculline (10 μM) and CGP-55845 (200 nM) to block NMDA, $GABA_A$ and $GABA_B$ receptor-mediated synaptic inputs respectively. Where relevant, 5-HT$_{1A}$ receptors were also blocked with WAY-100,635 (1 μM) prior to obtaining a stable baseline of at least 5 min and then examining the effect of 5-CT (10 μM) application, before a final period of wash and confirmation of

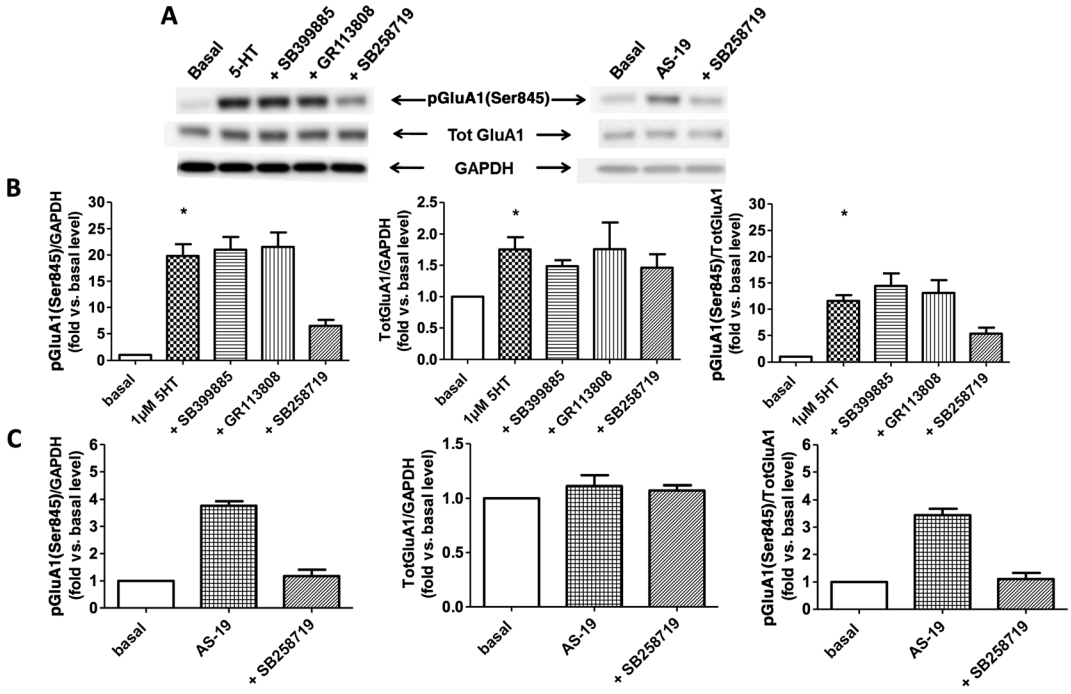

Figure 4

5-HT$_7$ receptor activation increases phosphorylation of GluA1 at Ser^{845} in hippocampal neurones. (A) Representative immunoblots of hippocampal neurones treated for 15 min with vehicle (DMSO 0.1%), GR113808 (1.0 μM; 5-HT$_4$ receptor antagonist), SB399885 (1.0 μM; 5-HT$_6$ receptor antagonist) or SB258719 (10 μM; 5-HT$_7$ receptor antagonist) followed by treatment with 5-HT (1 μM; left-hand panel) or AS-19 (1.0 μM; right-hand panel) for 5 min. (B, C) Quantification of pGluA1(Ser^{845}) and total GluA1. Ratio of pGluA1(Ser^{845})/GAPDH, total GluA1/GAPDH and pGluA1(Ser^{845})/total GluA1 are expressed as fold increase ±SEM with respect to basal levels from seven (5-HT), six (5-HT plus SB258719), four (AS-19) or three independent experiments. *$P < 0.05$, versus basal; Mann–Whitney *U*-test.

AMPA-mediated responses with NBQX (10 μM). In current clamp experiments, a minimum of two stable responses were obtained to AMPA application (10–20 μM, 2–6 s) in the presence of WAY-100,635 (1 μM) and tetrodotoxin (1 μM), before repeating in the presence of 5-CT (10 μM), a period of wash and, where possible, perfusion of SB258719 (20 μM) and a further 5-CT response examination. After completion of experiments, slices were fixed in 4% paraformaldehyde for a minimum of 48 h, before clearing with DMSO (>4 h), and visualisation of recorded cells using fluorescence microscopy to confirm their location within the CA3 pyramidal layer and characteristic morphology.

Data and statistical analysis

The data and statistical analysis in this study comply with the recommendations on experimental design and analysis in pharmacology (Curtis *et al.*, 2015). Where variance is indicated, data shown are means ± SEM. Drug concentration–response curves were fitted to a four parameter logistic equation using GraphPad Prism 5 (GraphPad Software Inc., San Diego, CA, USA). Agonist potency was expressed as pEC$_{50}$ (−log EC$_{50}$). The inhibition of antagonists was expressed as the pIC$_{50}$ (−logIC$_{50}$), where IC$_{50}$ represents the concentration of drug inhibiting 50% of agonist maximal response. pK$_B$ values for antagonists were determined using the equation pK$_B$ = (−log([antagonist]/(concentration ratio − 1)) where concentration ratio = ratio of the agonist EC$_{50}$ in the presence and absence of the antagonist.

For biochemical assays, where required, normalisation was a % change from the control group's individual value for a given experiment with individual values and then used to generate means ± SEM. Statistical analysis was only performed if the *n*-value was 5 or greater. Where more than two groups were compared, a Kruskal–Wallis ANOVA was performed. If $P < 0.05$ from the Kruskal–Wallis ANOVA or where just two groups were to be compared, a Mann–Whitney *U*-test was performed with $P < 0.05$ considered a statistically significant difference between groups.

Analysis of electrophysiological data was carried out using Clampfit 9.1 software (Molecular Devices LLC). For voltage clamp data, the mean maximum electrically-evoked EPSC amplitude measured from a minimum of five consecutive sweeps (60 s) was compared with a temporally matched period during the peak response to 5-CT. For current clamp data, the AUC (in V·ms^{-1}) of AMPA-evoked responses was the primary measurement; the baseline was taken as the response immediately preceding 5-CT perfusion. All data are represented as mean ± SEM. Comparisons between treatment periods were made using the paired Student's *t*-test. Probability (*P*) values <0.05 were considered significant.

Materials

5-HT, forskolin, papaverine and tetrodotoxin were purchased from Sigma-Aldrich, St. Louis, MO, USA; 5-CT, AMPA, AP-5, AS-19, bicuculline, CGP-55845, GR113808, H89, rolipram,

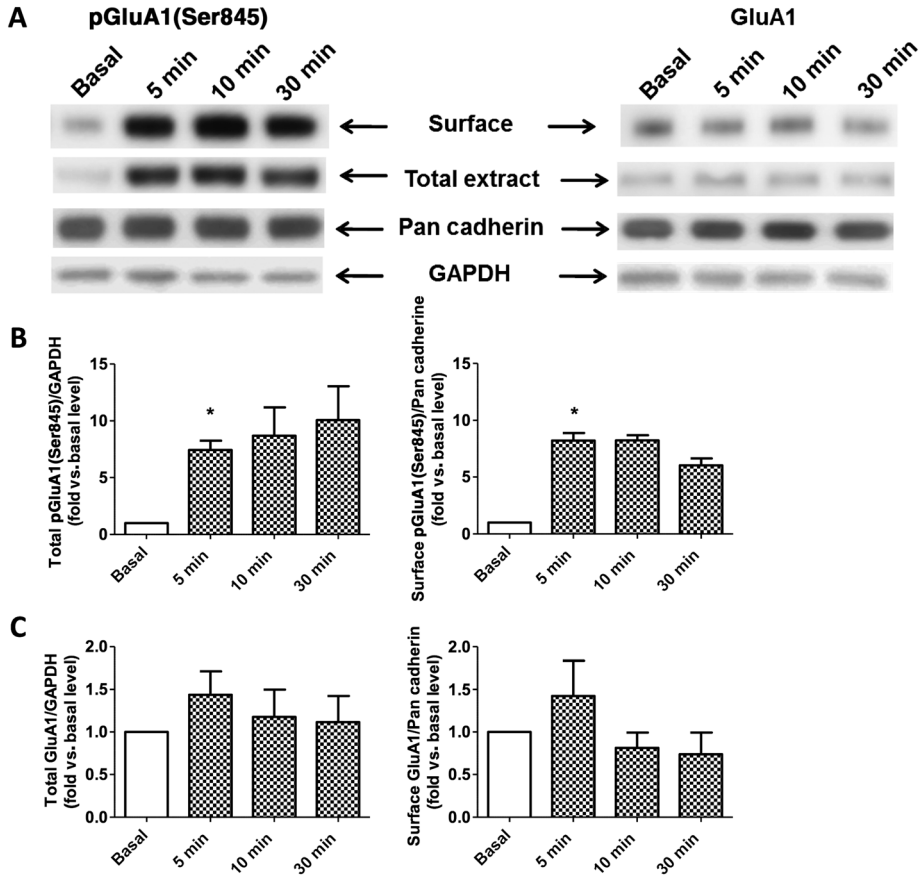

Figure 5

Ability of 5-HT to affect cell surface membrane expression of pGluA1(Ser^{845}). (A) Representative immunoblots of neurones treated with 5-HT (1 μM) for 5–30 min. (B,C) Quantification of pGluA1(Ser^{845}) and total GluA1 in the total cell extract (left) and in the surface fraction (right). Amount of proteins was normalized using GAPDH and pan cadherin in the total cell extract and in the cell surface fraction respectively. Values are expressed as fold increase ±SEM with respect to basal levels from seven [5-HT (5 min)] or four independent experiments *$P < 0.01$, 5-HT (5 min) versus basal; Mann–Whitney *U*-test.

SB258719, SB399885 and WAY-100,635 were from Tocris Bioscience, Ellisville, MO, USA. Laboratory reagents were from Sigma-Aldrich unless otherwise specified. Cell culture reagents were purchased from Gibco/Invitrogen (Life Technologies, Paisley, UK), except where otherwise indicated.

Results

5-HT$_7$ receptor mRNA expression in primary culture of hippocampal cells

The purity of primary cell cultures after 8–10 days *in vitro* was evaluated by immunocytochemistry for the neuronal marker NeuN and the astrocyte marker GFAP; the percentage of hippocampal NeuN- and GFAP-positive cells vs. DAPI-stained cells was around 80% and 10%, respectively (Supporting Information Figure S1). At the same end-point of 8–10 days *in vitro*, expression of 5-HT$_7$ receptor mRNA was evident by RT-PCR with appropriate sized product detected from cultured hippocampal cells (and also cultured cerebral cortex cells and adult hippocampus; Figure 1). Hereafter the hippocampal primary cells enriched considerably for neurones using appropriate culture conditions will be termed hippocampal neurones.

Ability of 5-HT to increase intracellular cAMP levels in hippocampal neurones and pharmacological definition of the receptor

5-HT displayed a concentration-dependent ability to increase cAMP levels in hippocampal neurones (pEC$_{50}$ of 7.2 ± 0.2; Hill slope of 1.2 ± 0.2; Figure 2A). Neither the selective 5-HT$_4$ receptor antagonist, GR113808, nor the selective 5-HT$_6$ receptor antagonist, SB399885 (either at concentrations up to 1.0 μM), prevented the ability of a sub-maximal concentration of 5-HT (100 nM) to increase cAMP levels (the increase in cAMP levels evident at the relatively high micromolar concentrations of SB399885 may be a consequence of engagement with additional receptors; Hirst *et al.*, 2006). In contrast, the selective 5-HT$_7$ receptor antagonist, SB258719, prevented the ability of 5-HT (100 nM) to increase cAMP levels in a concentration-dependent manner (pIC$_{50}$ of 7.95 ± 0.09, $n = 3$; Figure 2B). Furthermore, SB258719 displayed competitive antagonism of the 5-HT-evoked response (pK$_b$ of 8.23 ± 0.1; Figure 2C).

Influence of 5-HT$_7$ receptors upon pCREB levels in hippocampal neurones

5-HT (1 μM) increased the relative pCREB levels (pCREB :- CREB ratio) above basal levels although the signal was transient (evident at 5 min of incubation with 5-HT but not at 10 min and longer; Figure 3A). Prior incubation with SB258719 (100 nM to 10 μM) inhibited the ability of 5-HT (5 min) to increase relative pCREB levels in a concentration-dependent manner (Figure 3B).

5-HT (1 μM) failed to modify phosphorylated p38 MAPK levels in the hippocampal neurones (Supporting Information Figure S2). This contrasted the ability of 5-HT (1 μM) to increase phosphorylated p38 MAPK levels in rat primary astrocytes (Supporting Information Figure S2), the latter being consistent with previous studies (e.g. Lieb *et al.*, 2005).

Influence of 5-HT$_7$ receptors upon GluA1 expression and post-translational modification in hippocampal neurones

In hippocampal neurones, either 5-HT (1 μM; 5 min) or forskolin (10 μM; 5 min) increased the relative total GluA1 protein level and to a greater extent the relative protein level of pGluA1(Ser^{845}) (Supporting Information Figures S3 and 4).

The prior application of either GR113808 (up to10 μM) or SB399885 (up to 10 μM) failed to block the effects of 5-HT on the relative total GluA1 or pGluA1(Ser^{845}) protein levels, whereas SB258719 (10 μM) reduced the ability of 5-HT to increase relative pGluA1(Ser^{845}) protein levels (Figure 4) although not total GluA1 protein levels (Figure 4B).

Similar to 5-HT, the selective 5-HT$_7$ receptor agonist AS-19 (1 μM) increased relative levels of pGluA1(Ser^{845}) and the action of AS-19 was prevented completely by prior application of SB258719 (10 μM; Figure 4). However, AS-19 (1 μM) did not increase total GluA1 protein levels (Figure 4C). This lack of activity associated with AS-19 and the failure of SB258719 (10 μM) to prevent the 5-HT-induced increase in total GluA1 protein levels suggest that the latter effect was not mediated via the 5-HT$_7$ receptor.

Influence of 5-HT$_7$ receptors upon cell surface GluA1 AMPA receptor expression in hippocampal neurones

Treatment of hippocampal neurones with 5-HT (1 μM) increased cell surface membrane expression of pGluA1(Ser^{845}) for the three time points investigated (5, 10 and 30 min; Figure 5). In contrast, no difference in the cell surface levels of GluA1 was detected (Figure 5).

The ability of 5-HT (1 μM) to increase cell surface membrane expression of pGluA1(Ser^{845}) was prevented by prior application of either SB258719 (10 μM; Figure 6) or the PKA inhibitor, H89 (10 μM; Figure 6). As demonstrated in other experiments, SB258719 (10 μM) also inhibited the 5-HT-induced increase in pGluA1(Ser^{845}) in the total cell extracts, as did H89 (10 μM; Figure 6).

Ability of PDE$_4$ and PDE$_{10}$ to regulate 5-HT-induced pGluA1(Ser^{845}) in hippocampal neurones

In hippocampal neurones, either the PDE4 inhibitor, rolipram (10 μM), or the PDE10 inhibitor, papaverine (10 μM), increased

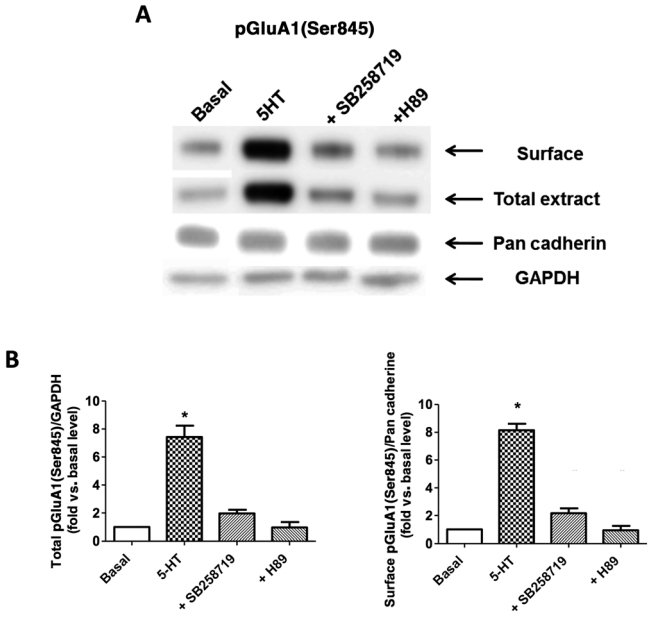

Figure 6

The 5-HT$_7$ receptor increases cell surface expression of pGluA1(Ser^{845}) via PKA in hippocampal neurones. (A) Representative immunoblots of hippocampal neurones treated with vehicle (basal and 5-HT) SB258719 (10 μM) or H89 (10 μM) for 15 min followed by addition of 5-HT (1 μM) or vehicle (basal) treatment for 5 min. (B) Quantification of pGluA1(Ser^{845}) levels in the total cell extracts and in the cell surface fractions. Amount of proteins was normalized using GAPDH and pan cadherin in the total extract and in the cell surface fraction respectively. Values are expressed as fold increase ±SEM with respect to basal levels from seven (5-HT) or three independent experiments. *$P < 0.01$, 5-HT versus basal; Mann–Whitney *U*-test.

levels of pGluA1(Ser^{845}) (Supporting Information Figure S4), which were further increased by combination with 5-HT (1.0 μM) to levels above those detected with 5-HT (1 μM) alone (Supporting Information Figure S4). In contrast, neither rolipram nor papaverine altered levels of total GluA1 when applied alone or in combination with 5-HT (Supporting Information Figure S4).

Ability of the 5-HT$_{1A/7}$ receptor agonist 5-CT to alter the firing pattern of hippocampal CA3 neurones in vivo

Extracellular recordings were performed in anaesthetized rats (n = 12) examining the effects of iontophoretic administration of the 5-HT$_{1A/7}$ receptor agonist, 5-CT (for electrode placement see Supporting Information Figure S5). In all, recordings were made from 16 hippocampal CA3 pyramidal neurones, of which 50% (8/16) were active (firing rate of 7.9 ± 3.0 Hz), whilst the remaining were quiescent. In seven of these active neurones, 5-CT administration was tested on baseline activity, with neuronal activity significantly reduced from 15.1 ± 2.8 to 9.7 ± 3.7 Hz in four of these seven neurones and activity increasing from 0.8 ± 0.4 to 4.9 ± 1.7 Hz in the remaining three neurones (Figure 7A and C). To remove the potentially confounding effect of 5-HT$_{1A}$ receptor activation by 5-CT, the selective 5-HT$_{1A}$ receptor antagonist, WAY-

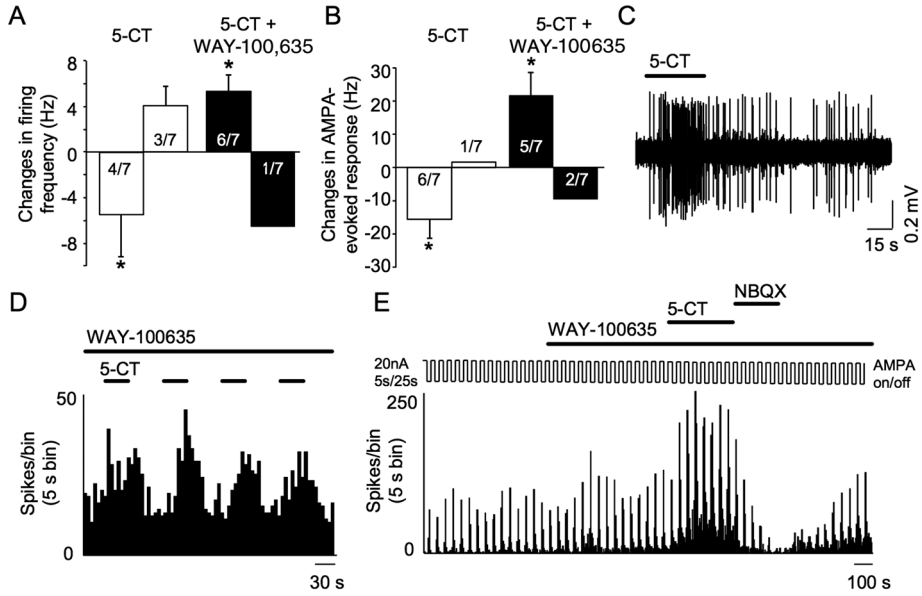

Figure 7

Iontophoretic administration of the 5-$HT_{1A/7}$ receptor agonist 5-CT induced a predominant excitation in the baseline and AMPA-induced firing of hippocampal CA3 pyramidal neurones in the presence of the 5-HT_{1A} receptor antagonist WAY-100,635, *in vivo*. (A) Group data revealed a mixed excitatory/inhibitory response to 5-CT administration on baseline neurone firing in the absence of WAY-100,635, which was modified to an almost exclusively excitatory response during 5-HT_{1A} receptor blockade; neurone numbers are overlaid histograms of change in firing rate (in Hz). (B) Similarly, in the absence of WAY-100,635, 5-CT application depressed AMPA-evoked firing, whereas in the presence of WAY-100,635, 5-CT predominantly enhanced AMPA-evoked bursts of activity; neurone numbers are overlaid histograms of change in firing rate (in Hz). (C,E) Typical examples of 5-CT inducing an increase in baseline neuronal activity in the absence of WAY-100,635 (C), an increase in neuronal activity in the presence of WAY-100,635 (D) and an enhancement of AMPA-evoked firing in the presence of WAY-100,635, with demonstration of AMPA receptor mediation using NBQX also shown (E). *$P < 0.05$ versus basal levels; paired Student's *t*-test.

100,635, was applied to seven neurones, which revealed an almost exclusively excitatory response to 5-CT; the firing rate of six of these seven neurones was increasing significantly from a mean of 6.2 ± 2.2 to 11.5 ± 2.5 Hz ($P < 0.05$, $n = 6$; Figure 7A and D). Only a single neurone (1/7) was activity reduced (from 12.7 to 6.2 Hz; Figure 7A).

The effects of 5-CT were also examined on bursts of action potential firing of hippocampal CA3 pyramidal neurones induced by cyclical administration of AMPA. When tested with 5-CT alone, AMPA-evoked firing was significantly reduced in the majority (6/7) of neurones (from 29.0 ± 12.0 to 13.6 ± 6.2 Hz; Figure 7B) and in the remaining neurone firing increased from 6.3 to 7.9 Hz (Figure 7B). However, in the presence of the selective 5-HT_{1A} receptor antagonist WAY-100,635, a predominant excitatory action of 5-CT was revealed, with AMPA-induced neuronal firing increased significantly in five of these seven neurones (from 28.6 ± 8.7 to 50.1 ± 13.8 Hz; Figure 7B and E) with the activity of the remaining two neurones being reduced from 13.2 to 3.9 Hz (Figure 7B).

Ability of the 5-HT_7 receptor to modify synaptic input into hippocampal CA3 pyramidal neurones in vitro

To determine whether 5-HT_7 receptor activation could modify the magnitude of AMPA receptor-mediated synaptic input to CA3 pyramidal neurones, whole-cell patch clamp recordings were performed from rat hippocampal slices, electrically stimulating mossy fibre inputs to evoke EPSCs (for electrode placement, see Supporting Information Figure S5). In the presence of the 5-HT_{1A} receptor antagonist, WAY-100,635 (1.0 μM), the 5-$HT_{1A/7}$ receptor agonist, 5-CT (10 μM), revealed a mixed response with EPSC amplitude reduced to 62.4 ± 1.6% of control levels in three of the nine neurones (from 77.2 ± 23.0 to 48.8 ± 15.6 pA; Figure 8A, C top and D) and enhanced to 150.8 ± 14.5% of control levels in six of the nine neurones (from 69.6 ± 15.2 to 101.9 ± 20.5 pA; $P < 0.05$, $n = 6$; Figure 8B, C bottom and D). Both these responses partially recovered to pre-5-CT application levels upon washout of 5-CT (to 72.4 ± 24.3 and 86.2 ± 17.5 pA respectively). EPSCs were confirmed as AMPA receptor mediated via administration of the selective AMPA receptor antagonist, NBQX (10 μM), which abolished EPSC amplitude (Figure 8A–D).

Further patch clamp experiments were performed to determine the effects of 5-HT_7 receptor activation upon isolated postsynaptic AMPA receptor-mediated activity by examining the effects of 5-CT (10 μM) administration, in the presence of tetrodotoxin (1 μM) and WAY-100,635 (1 μM), upon short periods of depolarisation induced by brief perfusion with AMPA (20 μM). These current clamp experiments revealed an almost exclusive augmentation of AMPA-induced depolarisation by 5-CT (10 μM), with the AUC of eight neurones enhanced significantly from 1169 ± 167 to 1827 ± 284 $V \cdot ms^{-1}$ (156.8 ± 10.4% of control; $P < 0.01$, $n = 8$; Figure 9A, B and D), with recovery following washout of 5-CT (to 1262 ± 236 $V \cdot ms^{-1}$, 104.7 ± 10.0% of pre-5-CT application;

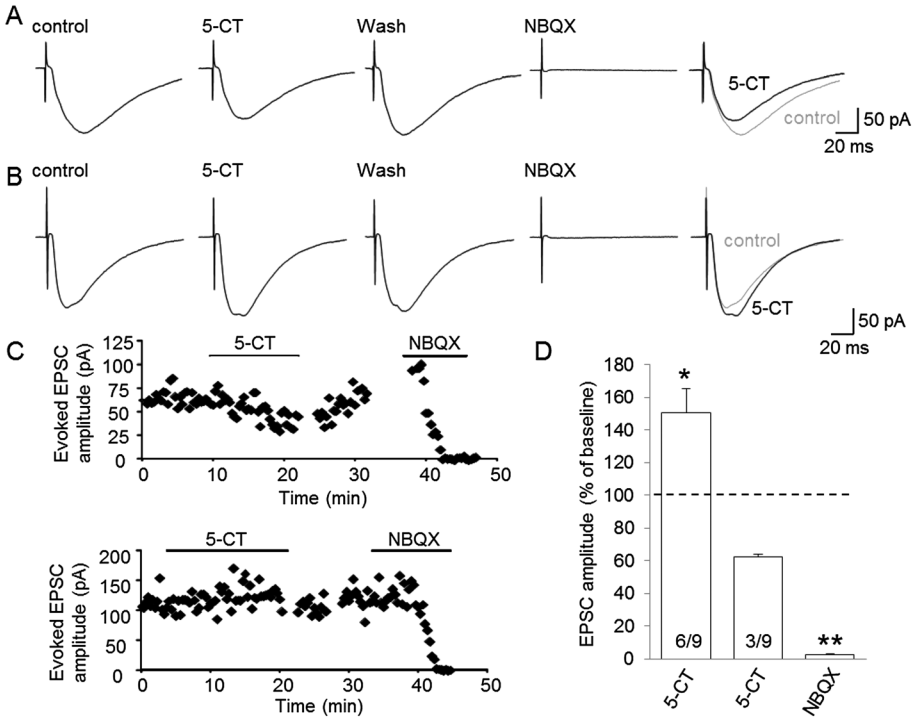

Figure 8

The 5-HT$_{1A/7}$ receptor agonist 5-CT induced both enhancements and reductions in the amplitude of electrically evoked AMPA-mediated EPSCs, in hippocampal CA3 pyramidal neurones in the presence of the 5-HT$_{1A}$ receptor antagonist WAY-100,635, *in vitro*. Typical CA3 pyramidal neurone in which 5-CT induced a reduction (A) and an enhancement (B) in the magnitude of EPSCs, recorded in the presence of AP-5, bicuculline, CGP55845 and WAY-100,635, with typical traces during baseline, 5-CT, wash and NBQX shown (each trace is the average of five sweeps). (C) Scatter plots representing EPSC amplitude over time of two CA3 pyramidal neurones in which 5-CT induced a reduction (top) and an enhancement (bottom), with the subsequent administration of NBQX also shown. (D) Group data of the effect of 5-CT and NBQX on AMPA-mediated EPSC activity in the presence of WAY-100,635; neurone numbers are overlaid histograms of change in EPSC amplitude as a percentage of baseline. *$P < 0.05$ versus basal levels; paired Student's *t*-test.

Figure 9D). In three neurones, AUC analysis revealed a similar mean control 5-CT increase to 157.2 ± 4.7% of AMPA responses ($n = 3$), which was reduced to 111.0 ± 14.7%, when repeated in the added presence of the 5-HT$_7$ receptor antagonist SB258719 (1 μM; Figure 9C and D).

Discussion

The present studies originated to better understand the mechanisms that might underlie the ability of the 5-HT$_7$ receptor to modulate glutamate-mediated neurotransmission (Bacon and Beck, 2000; Bickmeyer *et al.*, 2002; Gill *et al.*, 2002; Tokarski *et al.*, 2003, 2005; Costa *et al.*, 2012), which may have relevance to the ability of the 5-HT$_7$ receptor to modulate memory and learning (Meneses, 2004; Perez-Garcia and Meneses, 2005; Ballaz *et al.*, 2007; Eriksson *et al.*, 2008; Sarkisyan and Hedlund, 2009; Horisawa *et al.*, 2011; Waters *et al.*, 2012; Freret *et al.*, 2014) and relevant physiological phenomena such as long-term potentiation.

Initially, our investigations used primary cultures of rat hippocampus under suitable conditions to favour the culture of neurones. The cultured hippocampal neurones expressed 5-HT$_7$ receptor transcripts, and pharmacological studies demonstrated that activation of the 5-HT$_7$ receptor increased cAMP levels as well as the phosphorylation of the downstream signalling transcription factor, CREB. A key finding in the present study was that 5-HT$_7$ receptor activation signalled via the cAMP-dependent kinase, PKA, by phosphorylation of Ser^{845} within the C-terminal tail of the GluA1 AMPA receptor subunit. This post-transcriptional modification promoted expression of the pGluA1(Ser^{845}) subunit in the neuronal surface membrane.

Glutamate AMPA receptors are the primary means of relaying excitatory synaptic neurotransmission, and regulation of their function alters synaptic plasticity and associated memory function. It is well established that phosphorylation of AMPA receptor subunits modifies their activity (Song and Huganir, 2002). The GluA1 subunit forms homomeric receptors and also contributes a major component of the predominant heteromeric AMPA receptor (GluA1/2) in the hippocampus (Lu *et al.*, 2009). The GluA1 AMPA receptor subunit contains two phosphorylation sites, Ser^{831} and Ser^{845}. The Ser^{831} is a substrate for calcium/calmodulin-dependent protein kinase and PKC (Roche *et al.*, 1996; Barria *et al.*, 1997; Mammen *et al.*, 1997), whereas Ser^{845} is a substrate for PKA (Roche *et al.*, 1996). Relevant to the present study, phosphorylation of Ser^{845} within

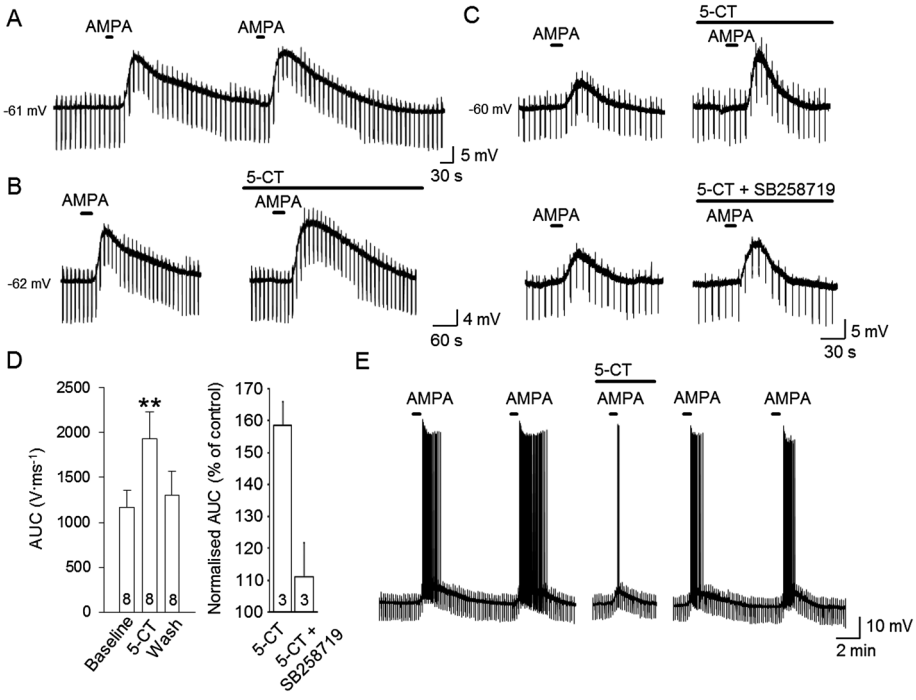

Figure 9

The 5-$HT_{1A/7}$ receptor agonist 5-CT enhanced excitatory responses of hippocampal CA3 pyramidal neurons *in vitro* induced by short-term application of AMPA, in the presence of the 5-HT_{1A} receptor antagonist and the sodium channel blocker, WAY-100,635 and tetrodotoxin respectively. The 5-CT-induced enhancement was antagonized by the 5-HT_7 receptor antagonist, SB258719. (A–C) CA3 pyramidal neurones recorded in current clamp in the presence of WAY-100,635 and tetrodotoxin (TTX) demonstrating (A) repeatable AMPA perfusion-induced depolarizations, (B) the enhancement in AMPA responses induced by 5-CT and (C) the reduced enhancement in the added presence of SB258719. (D) Left: group data of the effect of 5-CT on the AMPA-evoked excitation of six CA3 pyramidal neurones, in the presence of WAY-100,635 and TTX and measured using AUC analysis. Right: group data of the normalized increase in AMPA-evoked responses induced by 5-CT in the absence and presence of SB258719 recorded from three of these neurons. (E) A CA3 pyramidal neurone in which the effect of AMPA has been examined in the absence of WAY-100-635 and TTX. $^{**}P < 0.01$ versus basal levels; paired Student's *t*-test.

GluA1 subunits by directly enhancing cAMP levels (via either direct stimulation of adenylate cyclase by forskolin or inhibition of PDE by rolipram) promotes cell surface expression of the pGluA1(Ser^{845}) subunit (Esteban *et al.*, 2003; Oh *et al.*, 2006) and promotes AMPA receptor function (Roche *et al.*, 1996; Lee *et al.*, 2000; Oh *et al.*, 2006; He *et al.*, 2009; Makino and Malinow, 2009). In the present studies, activation of the 5-HT_7 receptor increased cell surface expression of pGluA1(Ser^{845}) via a PKA-dependent mechanism, consistent with the 5-HT_7 receptor elevating cAMP levels. The involvement of the 5-HT_7 receptor was indicated by a number of lines of evidence. Thus, 5-HT_7 receptor transcripts were expressed by the primary neurones in culture, and their functional involvement was verified pharmacologically by the action of the selective 5-HT_7 receptor agonist AS-19 at a just-maximal concentration to activate the 5-HT_7 receptor (1 μM; Brenchat *et al.*, 2009), action comparable to that of 5-HT (pEC_{50} = 7.2). The apparent lower efficacy of AS-19 compared with 5-HT may reflect the partial agonist action of AS-19 demonstrated in other assays *in vitro* (Brenchat *et al.*, 2009). Furthermore, the relatively selective 5-HT_7 receptor antagonist, SB258719 (Thomas *et al.*, 1998, 1999), antagonized the 5-HT-evoked responses. SB258719 also displayed competitive receptor antagonism of the 5-HT-induced increase in cAMP levels within the primary hippocampal cultures generating a pK_b of 8.23, consistent with the affinity of SB258719 for the 5-HT_7 receptor (Thomas *et al.*, 1998, 1999). Furthermore, two additional 5-HT receptor subtypes known to increase cAMP production, the 5-HT_4 and 5-HT_6 receptors, did not appear relevant to the responses detected in the present studies because the selective 5-HT_4 and 5-HT_6 receptor antagonists, GR113808 (Gale *et al.*, 1994) and SB399885 (Hirst *et al.*, 2006), failed to inhibit 5-HT-induced elevated cAMP levels in the hippocampal primary cell cultures at pharmacologically relevant concentrations (up to 1 μM). Involvement of cAMP was also indicated by the effect of PDE inhibition; thus, 5-HT_7 receptor-mediated phosphorylation of GluA1 was increased by the non-selective PDE4 and PDE10 inhibitors, rolipram and papaverine, respectively, with both PDE4 and PDE10 known to be expressed in hippocampus (Menniti *et al.*, 2006).

Consistent with the biochemical studies demonstrating that the 5-HT_7 receptor promoted expression of the pGluA1(Ser^{845}) subunit in the neuronal membrane of cells derived from all fields of the hippocampus, electrophysiological recordings in the CA3 field of the hippocampus *in vivo* revealed that 5-HT_7 receptor activation increased spontaneous activity and enhanced AMPA-induced increases in action potential firing. Furthermore, electrophysiological recordings *in vitro* demonstrated that whilst selective AMPA receptor-

mediated synaptic transmission via mossy fibre inputs to CA3 pyramidal neurones could be enhanced or depressed in the presence of 5-CT, AMPA-induced whole-cell postsynaptic currents were consistently increased by 5-HT$_7$ receptor activation.

The present studies confirmed the role of 5-HT$_7$ receptors in the regulation of CREB phosphorylation in hippocampal neurones (Mahgoub *et al.*, 2006). In contrast,5-HT had no effect on p38 MAPK in the same preparation, despite studies run in parallel that demonstrated that 5-HT did increase p38 MAPK phosphorylation in rat cortical astrocytes in culture, which also expressed 5-HT$_7$ receptor mRNA (data not shown). The latter is consistent with previous studies (Lieb *et al.*, 2005; Mahe *et al.*, 2005), and hence, our data suggest differential cell signalling for the 5-HT$_7$ receptor in neurones compared with astrocytes.

As well as the relatively short-term actions of 5-HT$_7$ receptors investigated in the present studies, relevant longer-term actions mediated via the 5-HT$_7$ receptor are also evident including elevation in glutamate levels *in vivo*, indicating enhanced excitatory synaptic tone (Canese *et al.*, 2015) and plastic neuronal remodelling (Kvachnina *et al.*, 2005; Kobe *et al.*, 2012; Speranza *et al.*, 2013; Canese *et al.*, 2015), which may underlie structural changes associated with memory formation.

Interestingly, a previous report suggests activation of the 5-HT$_{1B}$ receptor evokes calcium/calmodulin-dependent protein kinase-mediated phosphorylation of the GluA1 subunit at a further phosphorylation site in the C-terminus, Ser^{831}, which also contributes to 5-HT-induced potentiation of neurotransmission via a postsynaptic mechanism (Cai *et al.*, 2013).

In summary, the present study has demonstrated that 5-HT$_7$ receptor activation in rat hippocampal neurones signals a PKA-dependent phosphorylation of Ser^{845} within the GluA1 AMPA receptor subunit that results in increased levels of pGluA1(Ser^{845}) subunits within the neuronal membrane. These changes are likely to underlie the observed enhanced AMPA receptor-mediated neurotransmission within the rat hippocampus *in vitro* and *in vivo*.

Acknowledgements

This work was funded by a PhD studentship from GSK, Verona, Italy.

Author contributions

F.A., G.G., R.J., A.W. and M. van den T. performed the research. F.A., L.C., R.J, D.S. and N.B. designed the plan of research. All authors were involved in data analysis, interpretation of data and writing of the paper.

Conflict of interest

The authors declare no conflicts of interest.

Declaration of transparency and scientific rigour

This Declaration acknowledges that this paper adheres to the principles for transparent reporting and scientific rigour of preclinical research recommended by funding agencies, publishers and other organisations engaged with supporting research.

References

Alexander SPH, Davenport AP, Kelly E, Marrion N, Peters JA, Benson HE, *et al.* (2015a). The Concise Guide to PHARMACOLOGY 2015/16: G Protein-Coupled Receptors. Br J Pharmacol 172: 5744–5869.

Alexander SPH, Peters JA, Kelly E, Marrion N, Benson HE, Faccenda E, *et al.* (2015b). The Concise Guide to PHARMACOLOGY 2015/16: Ligand-gated ion channels. Br J Pharmacol 172: 5870–5903.

Alexander SPH, Fabbro D, Kelly E, Marrion N, Peters JA, Benson HE, *et al.* (2015c). The Concise Guide to PHARMACOLOGY 2015/16: Enzymes. Br J Pharmacol 172: 6024–6109.

Bacon WL, Beck SG (2000). 5-Hydroxytryptamine$_7$ receptor activation decreases slow afterhyperpolarization amplitude in CA3 hippocampal pyramidal cells. J Pharmacol Exp Ther 294: 672–679.

Ballaz SJ, Akil H, Watson SJ (2007). The 5-HT$_7$ receptor: role in novel object discrimination and relation to novelty-seeking behaviour. Neuroscience 149: 192–202.

Barria A, Derkach V, Soderling T (1997). Identification of the Ca^{2+}/calmodulin-dependent protein kinase II regulatory phosphorylation site in the alpha-3-hydroxyl-5-methyl-4-isoxazole-propionate type glutamate receptor. J Biol Chem 272: 32727–32730.

Bickmeyer U, Heine M, Manzke T, Richter DW (2002). Differential modulation of I(h) by 5-HT recetors in mouse CA1 hippocampal neurons. Eur J Neurosci 16: 209–218.

Bonaventure P, Aluisio L, Shoblock J, Boggs JD, Fraser IC, Lord B, *et al.* (2011). Pharmacological blockade of serotonin 5-HT7 receptor reverses working memory deficits in rats by normalizing cortical glutamate neurotransmission. PLoS One 6: e20210.

Brenchat A, Romero L, García M, Pujol M, Burgueño J, Torrens A, *et al.* (2009). 5-HT$_7$ receptor activation inhibits mechanical hypersensitivity secondary to capsaicin sensitization in mice. Pain 141: 239–247.

Cai X, Kallarackal AJ, Kvarta MD, Goluskin S, Gaylor K, Bailey AM, *et al.* (2013). Local potentiation of excitatory synapses by serotonin and its alteration in rodent models of depression. Nat Neurosci 16: 464–472.

Canese R, Zoratto F, Altabella L, Porcari P, Mercurio L, de Pasquale F, *et al.* (2015). Persistent modification of forebrain networks and metabolism in rats following adolescent exposure to a 5-HT$_7$ receptor agonist. Psychopharmacology (Berl) 232: 75–89.

Costa L, Trovato C, Musumeci SA, Catania MV, Ciranna L (2012). 5-HT$_{1A}$ and 5-HT$_7$ receptors differentially modulate AMPA receptor-mediated hippocampal synaptic transmission. Hippocampus 22: 790–801.

Curtis MJ, Bond RA, Spina D, Ahluwalia A, Alexander SPH, Giembycz MA, *et al.* (2015). Experimental design and analysis and their reporting: new guidance for publication in *BJP*. Br J Pharmacol 172: 3461–3471.

Eriksson TM, Golkar A, Ekstrom JC, Svenningsson P, Ogren SO (2008). 5-HT_7 receptor stimulation by 8-OHDPAT counteracts the impairing effect of 5-HT_{1A} receptor stimulation on contextual learning in mice. Eur J Pharmacol 596: 107–110.

Esteban JA, Shi SH, Wilson C, Nuriya M, Huganir RL, Malinow R (2003). PKA phosphorylation of AMPA receptor subunits controls synaptic trafficking underlying plasticity. Nat Neurosci 6: 136–143.

Freret T, Paizanis E, Beaudet G, Gusmao-Montaigne A, Nee G, Dauphin F, *et al.* (2014). Modulation of 5-HT_7 receptor: effect on object recognition performances in mice. Psychopharmacology (Berl) 231: 393–400.

Fountoulakis KN, Gazouli M, Kelsoe J, Akiskal H (2015). The pharmacodynamic properties of lurasidone and their role in its antidepressant efficacy in bipolar disorder. Eur Neuropsychopharmacol 25: 335–342.

Gale JD, Grossman CJ, Whitehead JW, Oxford AW, Bunce KT, Humphrey PPA (1994). GR113808: a novel, selective antagonist with high affinity at the 5-HT_4 receptor. Br J Pharmacol 111: 332–338.

Gellynck E, Heyninck K, Andressen KW, Haegeman G, Levy FO, Vanhoenacker P, *et al.* (2013). The serotonin 5-HT_7 receptors: two decades of research. Exp Brain Res 230: 555–568.

Gill CH, Soffin EM, Hagan JJ, Davies CH (2002). 5-HT_7 receptors modulate synchronized network activity in rat hippocampus. Neuropharmacology 42: 82–92.

Gustafson EL, Durkin MM, Bard JA, Zgombick J, Branchek TA (1996). A receptor autoradiographic and in situ hybridization analysis of the distribution of the 5-HT_7 receptor in rat brain. Br J Pharmacol 117: 657–666.

He K, Song L, Cummings LW, Goldman J, Huganir RL, Lee HK (2009). Stabilisation of Ca2 + -permeable AMPA receptors at periynaptic sites by GluR1-S845 phosphorylation. Proc Natl Acad Sci U S A 106: 20033–20038.

Hirst WD, TO S, Rogers DC, Sunter D, Pugh P, Moss SF, *et al.* (2006). SB-399885 is a potent, selective 5-HT6 receptor antagonist with cognitive enhancing properties in aged rat water maze and novel object recognition models. Eur J Pharmacol 553: 109–119.

Horiguchi M, Huang M, Meltzer HY (2011). The role of 5-hydroxytryptamine$_7$ receptors in the phencyclidine-induced novel object recognition deficit in rats. J Pharmacol Exp Ther 338: 605–614.

Horisawa T, Ishibashi T, Nishikawa H, Enomoto T, Toma S, Ishiyama T, *et al.* (2011). The effects of selective antagonists of serotonin 5-HT_7 and 5-HT_{1A} receptors on MK-801-induced impairment of learning and memory in the passive avoidance and Morris water maze tests in rats: mechanistic implications for the beneficial effects of the novel atypical antipsychotic lurasidone. Behav Brain Res 220: 83–90.

Hoyer D, Clarke DE, Fozard JR, Hartig PR, Martin GR, Mylecharane EJ, *et al.* (1994). International Union of Pharmacology classification of receptors for 5-hydroxytryptamine (serotonin). Pharmacol Rev 46: 157–204.

Kilkenny C, Browne W, Cuthill IC, Emerson M, Altman DG, NC3Rs Reporting Guidelines Working Group (2010). Animal research: reporting in vivo experiments: the ARRIVE guidelines. Br J Pharmacol 160: 1577–1579.

Kobe F, Guseva D, Jensen TP, Wirth A, Renner U, Hess D, *et al.* (2012). 5-HT7R/G12 signaling regulates neuronal morphology and function in an age-dependent manner. J Neurosci 32: 2915–2930.

Kvachnina E, Liu G, Dityatev A, Renner U, Dumuis A, Richter DW, *et al.* (2005). 5-HT_7 receptor is coupled to G alpha subunits of heteromeric G12-protein to regulate gene transcription and neuronal morphology. J Neurosci 25: 7821–7830.

Lee HK, Barbarosie M, Kameyama K, Bear MF, Huganir RL (2000). Regulation of distinct AMPA receptor phosphorylation sites during bidirectional synaptic plasticity. Nature 405: 955–959.

Lieb K, Biersack L, Waschbisch A, Orlikowski S, Akundi RS, Candelario-Jalil E, *et al.* (2005). Serotonin via 5-HT_7 receptors activates p38 mitogen-activated protein kinase and protein kinase C epsilon resulting in interleukin-6 synthesis in human U373 MG astrocytoma cells. J Neurochem 93: 549–559.

Lu W, Shi Y, Jackson AC, Bjorgan K, During MJ, Sprengel R, *et al.* (2009). Subunit composition of synaptic AMPA receptors revealed by single-cell genetic aproach. Neuron 62: 254–268.

Mahe C, Loetscher E, Dev KK, Bobirnac I, Otten U, Schoeffter P (2005). Serotonin 5-HT_7 receptors coupled to induction of interleukin-6 in human microglial MC-3 cells. Neuropharmacology 49: 40–47.

Mahgoub MA, Sara Y, Kavalali ET, Monteggia LM (2006). Reciprocal interaction of serotonin and neuronal activity in regulation of cAMP-responsive element-dependent gene expression. J Pharmacol Exp Ther 317: 88–96.

Makino H, Malinow R (2009). AMPA receptor incorporation into synapses during LTP: the role of lateral movement and exocytosis. Neuron 64: 381–390.

Mammen AL, Kameyame K, Roche KW, Huganir RL (1997). Phosphorylation of the alpha-3-hydroxyl-5-methyl-4-isoxazole-propionic acid receptor GluR1 subunit by calcium/calmodulin-dependent kinase II. J Biol Chem 272: 32528–32533.

McGrath JC, Lilley E (2015). Implementing guidelines on reporting research using animals (ARRIVE etc.): new requirements for publication in BJP. Br J Pharmacol 172: 3189–3193.

McLean SL, Woolley ML, Thomas D, Neill JC (2009). Role of 5-HT receptor mechanisms in sub-chronic PCP-induced reversal learning deficits in the rat. Psychopharmacology (Berl) 206: 403–414.

Meneses A (2004). Effects of the 5-HT_7 receptor antagonists SB-269970 and DR 4004 in autoshaping Pavlovian/instrumental learning task. Behav Brain Res 155: 275–282.

Mengod G, Cortés R, Vilaró MT, Hoyer D (2010). Distribution of 5-HT receptors in the central nervous system. In: Mueller C, Jacobs B (eds). Handbook of the Behavioral Neurobiology of Serotonin. Academic Press/Elsevier: Cambridge, MA, USA, pp. 123–138.

Menniti FS, Faraci WS, Schmidt CJ (2006). Phosphodiesterases in the CNS: targets for drug development. Nat Rev Drug Discov 5: 660–670.

Mnie-Filali O, Lambas-Senas L, Zimmer L, Haddjeri N (2007). 5-HT_7 receptor antagonists as a new class of antidepressants. Drug News Perspect 20: 613–618.

Neumaier JF, Sexton TJ, Yracheta J, Diaz AM, Brownfield M (2001). Localization of 5-HT7 receptors in rat brain by immunocytochemistry, in situ hybridisation, and agonist stimulated cFos expression. J Chem Neuroanat 21: 63–73.

Nikiforuk A, Kos T, Fijal K, Holuj M, Rafa D, Popik P (2013). Effects of the selective 5-HT_7 receptor antagonist SB-269970 and amisulpride on ketamine-induced schizophrenia-like deficits in rats. PLoS One 8: e66695.

Oh MC, Derkach VA, Guire ES, Soderling TR (2006). Extrasynaptic membrane trafficking regulated by GluR1 serine 845 phosphorylation primes AMPA receptors for long-term potentiation. J Biol Chem 281: 752–758.

Pawson AJ, Sharman JL, Benson HE, Faccenda E, Alexander SPH, Buneman OP, *et al.* (2014). The IUPHAR/BPS Guide to PHARMACOLOGY: an expert-driven knowledge base of drug targets and their ligands. Nucl Acids Res 42 (Database Issue): D1098–D1106.

Paxinos G, Watson C (1998). The rat brain in stereotaxic coordinates. Academic Press.

Perez-Garcia GS, Meneses A (2005). Effects of the potential 5-HT$_7$ receptor agonist AS19 in an autoshaping learning task. Behav Brain Res 163: 136–140.

Pickering AE, Spanswick D, Logan SD (1991). Whole-cell recordings from sympathetic preganglionic neurons in rat spinal cord slices. Neurosci Lett 130: 237–242.

Renner U, Zeug A, Woehler A, Niebert M, Dityatev A, Ditateva G, *et al.* (2012). Heterodimerization of serotonin receptors 5-HT$_{1A}$ and 5-HT$_7$ differentially regulates receptor signalling and trafficking. J Cell Sci 125: 2486–2499.

Roberts RJ, Krucker T, Levy CL, Slanina KA, Sutcliffe JG, Hedlund PB (2004). Mice lacking 5-HT receptors show specific impairments in contextual learning. Eur J Neurosci 19: 1913–1922.

Roche KW, O'Brien RJ, Mammen AL, Bernhardt J, Huganir RL (1996). Characterisation of multiple phosphorylation sites on the AMPA receptor GluR1 subunit. Neuron 16: 1179–1188.

Roth BL, Craigo SC, Choudhary MS, Uluer A, Monsma FJ, Shen Y, *et al.* (1994). Binding of the typical and atypical antipsychotic agents to 5-hydroxytryptamine$_6$ and 5-hydroxytryptamine$_7$ receptors. J Pharmacol Exp Ther 268: 1403–1410.

Sanchez C, Asin KE, Artigas F (2015). Vortioxetine, a novel antidepressant with multimodal activity: review of preclinical and clinical data. Pharmacol Ther 145: 43–57.

Sarkisyan G, Hedlund PB (2009). The 5-HT$_7$ receptor is involved in allocentric spatial memory formation processing. Behav Brain Res 202: 26–31.

Shen Y, Monsma FJ, Metcalf MA, Jose PA, Hamblin MW, Sibley DR (1993). Molecular cloning and expression of a 5-hydroxytryptamine$_7$ serotonin receptor subtype. J Biol Chem 268: 18200–18204.

Song I, Huganir RL (2002). Regulation of AMPA receptors during synaptic plasticity. Trends Neurosci 25: 578–588.

Speranza L, Chambery A, Di Domenico M, Crispino M, Severino V, Volpicelli F, *et al.* (2013). The serotonin receptor 7 promotes neurite outgrowth via ERK and Cdk5 signaling pathways. Neuropharmacology 67: 155–167.

Stowe RL, Barnes NM (1998). Selective labeling of 5-HT$_7$ receptor recognition sites in rat brain using [^{3}H]5-carboxamidotryptamine. Neuropharmacology 37: 1611–1619.

Thomas DR, Gittins SA, Collin LL, Middlemiss DN, Riley G, Hagan J, *et al.* (1998). Functional characterization of the human cloned 5-HT7 receptor (long form); antagonist profile of SB-258719. Br J Pharmacol 124: 1300–1306.

Thomas DR, Middlemiss DN, Taylor SG, Nelson P, Brown AM (1999). 5-CT stimulation of adenylyl cyclase activity in guinea-pig hippocampus: evidence for involvement of 5-HT7 and 5-HT1A receptors. Br J Pharmacol 128: 158–164.

Tokarski K, Zahorodna A, Bobula B, Grzegorzewska M, Pitra P, Hess G (2005). Repeated administration of citalopram and imipramine alters the responsiveness of rat hippocampal circuitry to the activation of 5-HT$_7$ receptors. Eur J Pharmacol 524: 60–66.

Tokarski K, Zahorodna A, Bobula B, Hess G (2003). 5-HT$_7$ receptors increase the excitability of rat hippocampal CA1 pyramidal neurones. Brain Res 993: 230–234.

Vasefi MS, Yang K, Li J, Kruk JS, Heikkila JJ, Jackson MF, *et al.* (2013). Acute 5-HT$_7$ receptor activation increases NMDA-evoked currents and differentially alters NMDA receptor subunit phosphorylation and trafficking in hippocampal neurons. Molecular Brain 6: 24.

Waeber C, Moskowitz MA (1995). Autoradiographic visualisation of [^{3}H]5-carboxamidotryptamine binding sites in the guinea pig and rat brain. Eur J Pharmacol 283: 31–46.

Waters KA, Stean TO, Hammond B, Virley DJ, Upton N, Kew JN, *et al.* (2012). Effects of the selective 5-HT$_7$ receptor antagonist SB-269970 in animal models of psychosis and cognition. Behav Brain Res 228: 211–218.

Zamanillo D, Sprengel R, Hvalby O, Jensen V, Burnashev N, Rozov A, *et al.* (1999). Importance of AMPA receptors for hippocampal synaptic plasticity but not for spatial learning. Science 284: 1805–1811.

Supporting Information

Additional Supporting Information may be found in the online version of this article at the publisher's web-site:

http://dx.doi.org/10.1111/bph.13432

Figure S1 Immunofluorescence staining of hippocampal cells following 8-10 days in culture. A: anti-NeuN staining for neurones. B: anti-GFAP staining for astrocytes. C: DAPI staining for nuclei. D: overlay of the different stains.

Figure S2 Failure of 5-HT to increase p38 MAP kinase phosphorylation in hippocampal neurones. Top: Time-dependent lack of effect of 5-HT (1.0 μM) upon p38 MAP kinase phosphorylation (forskolin [FSK; 10 μM] applied for 30 min). Data represent the mean ± SEM of three independent experiments and represent the % of basal levels (*$P < 0.05$ vs. basal levels; one-way ANOVA with post hoc Dunnett's test). Bottom: Ability of 5-HT (1.0 μM) to increase p38 MAP kinase phosphorylation in cortical astrocytes and antagonism by SB258719 (10 μM). Data represent the mean ± SEM from seven independent experiments (*$P < 0.05$ 5-HT vs. basal levels; #$P < 0.05$ 5-HT plus SB258719 vs. 5-HT; Kruskal-Wallis ANOVA with Mann-Whitney U test).

Figure S3 Ability of the 5-HT or forskolin to increase phosphorylation of the AMPA receptor subunit, GluA1 at Ser^{845}), in hippocampal neurones. A: Representative immunoblots from cells treated with 5-HT (1.0 μM) or forskolin (10 μM) for 5 min. B: Quantification of pGluA1(Ser^{845})/GAPDH ratio, total GluA1/GAPDH ratio and pGluA1(Ser^{845})/total GluA1 ratio. Ratios are expressed as mean fold increase ± SEM with respect to basal levels from three independent experiments.

Figure S4 Ability of phosphodiesterase inhibition to modify the 5-HT$_7$ receptor-mediated increase in expression of pGluA1(Ser^{845}) in hippocampal neurones. A: Representative immunoblots of neurones treated for 30 min with rolipram (10 μM) or papaverine (10 μM), followed by addition of 5-HT (1.0 μM) or vehicle for 5 min. B-C: Quantification of pGluA1(Ser^{845}) and total GluA1 for the effects of rolipram (B) and papaverine (C). Ratio of pGluA1(Ser^{845})/GAPDH, total GluA1/GAPDH and pGluA1(Ser^{845})/total GluA1 are expressed as fold increase ± SEM with respect to basal levels from four (B: 5-HT and 5-HT plus rolipram) or three independent experiments.

Figure S5 Histologically marked recording sites from electrophysiological experiments. A: Schematic depicting the hippocampus, the CA3 region, and the approximate positioning of recording electrodes for *in vitro* and *in vivo* experiments. B: A light microscope image of a cryosectioned hippocampus recovered from an *in vivo* electrophysiological experiment in which the recording site has been marked by iontophoretic administration of the dye Chicago Sky Blue (blue dot; arrow). C: Brightfield and fluorescent (D) images of a typical Lucifer yellow-filled CA3 pyramidal neurone from which patch-clamp recordings were made.